



This is a repository copy of *Palaeoenvironmental reconstruction of the alluvial landscape of Neolithic Çatalhöyük, central southern Turkey : the implications for early agriculture and responses to environmental change*.

White Rose Research Online URL for this paper:
<http://eprints.whiterose.ac.uk/124237/>

Version: Accepted Version

Article:

Ayala, G., Wainwright, J., Walker, J. et al. (4 more authors) (2017) Palaeoenvironmental reconstruction of the alluvial landscape of Neolithic Çatalhöyük, central southern Turkey : the implications for early agriculture and responses to environmental change. *Journal of Archaeological Science*, 87. pp. 30-43. ISSN 0305-4403

<https://doi.org/10.1016/j.jas.2017.09.002>

Article available under the terms of the CC-BY-NC-ND licence
(<https://creativecommons.org/licenses/by-nc-nd/4.0/>)

Reuse

This article is distributed under the terms of the Creative Commons Attribution-NonCommercial-NoDerivs (CC BY-NC-ND) licence. This licence only allows you to download this work and share it with others as long as you credit the authors, but you can't change the article in any way or use it commercially. More information and the full terms of the licence here: <https://creativecommons.org/licenses/>

Takedown

If you consider content in White Rose Research Online to be in breach of UK law, please notify us by emailing eprints@whiterose.ac.uk including the URL of the record and the reason for the withdrawal request.



eprints@whiterose.ac.uk
<https://eprints.whiterose.ac.uk/>

1
2
3
4
5
6
7
8
9
10
11
12
13
14
15
16
17
18
19
20
21
22
23
24
25

PALAEOENVIRONMENTAL RECONSTRUCTION OF THE ALLUVIAL
LANDSCAPE OF NEOLITHIC ÇATALHÖYÜK, CENTRAL SOUTHERN
TURKEY: THE IMPLICATIONS FOR EARLY AGRICULTURE AND
RESPONSES TO ENVIRONMENTAL CHANGE

Gianna Ayala

Department of Archaeology, University of Sheffield

John Wainwright

Department of Geography, Durham University

Joanna Walker

Department of Geography, Durham University

Rachel Hodara

Haleakalā National Park

Jerry M Lloyd

Department of Geography, Durham University

Melanie Leng

BGS

Chris Doherty

Oxford University

Pre-publication copy

26 Abstract

27 Archaeological discussions of early agriculture have often used the Neolithic village of
28 Çatalhöyük in central southern Turkey as a key example of the restricting effect of
29 environment on agricultural production and organization. Central to these discussions is the
30 palaeoenvironmental reconstruction of the landscape surrounding the site. This paper presents
31 an important new dataset from an intensive coring programme undertaken between 2007 and
32 2013 in the immediate environs of the site, designed to improve significantly the spatial
33 resolution of palaeoenvironmental data. Using sediment analyses including organic content,
34 magnetic susceptibility, particle size, total carbon and nitrogen contents and carbon isotope
35 analysis, coupled with 3D modelling, we are able to present a new reconstruction of the
36 palaeotopography and sedimentary environments of the site. Our findings have major
37 implications for our understanding of Neolithic agricultural production and social practice.

38 We present four phases of environmental development. Phase 1 consists of the final phases of
39 regression of Palaeolake Konya in the later parts of the Pleistocene, dominated by erosion
40 due to wind and water that created an undulating surface of the marl deposited in the
41 palaeolake. Phase 2 occurs in the latest Pleistocene and early Holocene, and indicates
42 increased wetness, probably characteristic of a humid anabranching channel system, in which
43 there are localized pockets of wetter conditions. In Phase 3a, this infilling continues,
44 producing a flatter surface, and there are fewer pockets being occupied by wetter
45 conditions. The fluvial régime shifts from humid to dryland anabranching conditions. The
46 earliest period of occupation of the Neolithic East Mound coincides with this phase. Phase 3b
47 coincides with the shift of occupation to the West Mound in the Chalcolithic, when there is
48 evidence for a very localized wetter area to the southeast of the West Mound, but otherwise a
49 continuation of the dryland anabranching system. Finally, Phase 4 shows a shift to the pre-
50 modern style of fluvial environment, modified by channelization. This reanalysis
51 demonstrates the importance of extensive spatial sampling as part of geoarchaeological
52 investigations.

53 With this new evidence we demonstrate that the landscape was highly variable in time and
54 space with increasingly dry conditions developing from the early Holocene onwards. In
55 contrast to earlier landscape reconstructions that have presented marshy conditions during the
56 early Holocene that impacted agriculture, we argue that localized areas of the floodplain
57 would have afforded significant opportunities for agriculture closer to the site. In this way,

58 the results have important implications for how we understand agricultural practices in the
59 early Neolithic.

60

Pre-publication copy

61 Introduction

62 The site of Çatalhöyük (c.7400–6000 cal BCE: Bayliss et al. 2015, Cessford 2001) in central southern
63 Turkey has played a pivotal rôle in ongoing discussions regarding Neolithic settlement and the onset
64 of agriculture. The environmental reconstruction of the surrounding landscape of Çatalhöyük has been
65 at the centre of evolving archaeological debates about early agricultural communities and their
66 adaptation to environmental change (Sherratt 1980; Roberts 1991; Bogaard et al. 2014; Charles et al.
67 2014). Central to the palaeoenvironmental reconstruction of the past landscape is the characterisation
68 of the alluvial landscape in the vicinity of the site. The modern Çarşamba River flows close to the
69 edge of the site and extends southwards until the termination of the Konya Plain at limestone hills that
70 border the Taurus Mountains (Figure 1). Previous geoarchaeological research has characterized the
71 alluvial plain as a very marshy environment subject to significant seasonal flooding (Roberts et al.
72 1999; Boyer et al. 2006; Roberts and Rosen 2009) which has driven models of land use (Fairbairn
73 2005; Roberts and Rosen 2009). In particular, Roberts and Rosen (2009) have suggested that
74 agriculture during the Neolithic phases of the site would have been constrained by the marshy
75 conditions and could only have been undertaken upon the well-drained foothills up to 12 km from
76 site, which has significant implications for social and economic nature of settled life (see also Rosen
77 and Roberts 2005). These palaeoenvironmental models have been based on sedimentological data
78 derived from nine coring locations and trench sections near the tells as well as the investigation of 16
79 archaeological sites (four of which date from the Palaeolithic to Bronze Age) further away in the area
80 of Palaeolake Konya (Boyer 1999: 63; Boyer et al. 2006: 684; Boyer et al. 2007). Recent
81 interpretations of land use and *taskscape*s have attempted to integrate the sedimentological data with
82 on-site evidence, including but not limited to archaeobotanical and faunal remains, as well as clay
83 sourcing (Charles et al. 2014). At times this on-site environmental evidence fits well within the model
84 that suggests a dominantly wet landscape contemporary with the Neolithic settlement, but there is
85 increasing on-site palaeobotanical evidence that is beginning to challenge the pervasiveness of the
86 marsh environment (Bogaard et al. 2014; Charles et al. 2014).

87 As a consequence of these apparently conflicting interpretations of the Neolithic landscape, a further
88 campaign of geoarchaeological research was undertaken between 2007 and 2013, with the specific
89 aim of resolving these conflicts, using both more intensive and extensive sampling protocols. This
90 research provides an important body of data that raises significant questions about the validity of these
91 earlier palaeoenvironmental models and established ideas about early agriculture derived from them,
92 which would have required extensive time away from site for large numbers of the population to tend
93 fields. In this paper we provide data from a coring programme undertaken that targeted a further 29
94 coring locations within a radius of up to 1.6 km of Çatalhöyük to provide a more nuanced approach to
95 landscape reconstruction. The combination of sediment with isotope analysis and 3D modelling of the
96 stratigraphic sequence enables us to construct a more refined understanding of the hydrology and

97 resulting dynamic topography of the low-lying alluvial plain around this crucial time of early
98 agricultural society in the near East. This high-resolution environmental reconstruction provides direct
99 evidence of the Neolithic alluvial landscape from which we can advance archaeological discussions of
100 cultural response to environment and environmental change.

101

102

103 Regional Setting

104 Çatalhöyük is located in the Çumra District on the Konya Plain (Figure 1). The current climate is
105 defined by the Köppen-Geiger classification as BSk (de Meester 1970, 5; Kuzucuoğlu et al. 1999), or
106 cold semi-arid/steppe climate, having hot, dry summers and cold, wet winters. The majority of rainfall
107 at Çumra occurs between December and May, with an average annual precipitation of 350 mm, and
108 there is a considerable seasonal temperature range of over 20°C between the warmest and coolest
109 months. The climate regime can also be seen to include a three-month period of drought between July
110 and September, and throughout the year the winds in the basin come mainly from the north (Fontugne
111 et al. 1999).

112

113 The surface of the plain is fairly flat, with shoreline terraces and beaches rising up to 30 m above the
114 margins of the plain, suggesting that a fairly shallow, albeit expansive lake (>400 km²) occupied this
115 basin at its maximum extent. The basin has not been tectonically active in radiocarbon history, and so
116 recent stratigraphic sequences remain *in situ* (Roberts 1995).

117

118 Soil surveys by de Ridder (1965) and de Meester (1970), revealed that the basin is in places infilled
119 with in excess of 400 m of Quaternary marl sediments, testifying to the lengthy presence of a lake in
120 this location. More recently with greater water management the plain has dried, and three marshy
121 depressions within the basin, the Yarma marshes, the Konya marshes and the Hotamiş Lake, have
122 become desiccated leaving only the seasonal Sultaniye Lake and permanent Akgöl Lake as water-
123 holding depressions in the basin (Fontugne et al. 1999).

124

125 The plain today is dominated by irrigation agriculture, yet studies have shown that in recent history
126 *Artemisia* steppe and Chenopodiaceae were the chief plants present, with the volcanic soils having
127 open forests of *Quercus*, and limestone soils containing forests of *Pinus* and *Juniperus* (Kuzucuoğlu
128 et al. 1999; Fontugne et al. 1999). Further analysis of the palaeovegetation sequence is hindered by

129 limited palynological investigations in the Konya basin, which have been confined to deposits
130 collected from the Yarma and Akgöl basins, allowing few long vegetation sequences to be created,
131 and none locally to the Çarşamba fan (Bottema and Woldring 1984; Kuzucuoğlu et al. 1999;
132 Woldring and Bottema 2003; Roberts et al., 2016). Traditionally, pastoral grazing of sheep on the
133 plain has been crucial to the livelihoods of local populations which has undoubtedly controlled the
134 development of vegetation. Today though, grazing has moved onto the higher slopes surrounding the
135 plain (Russell and Martin, 2005).

136

137

138 Previous Palaeoenvironmental Research in the Konya Basin

139 The Konya Basin is a closed pluvial basin that has actively responded to changes in climate and
140 precipitation. Projects such as the KOPAL (*K*Onya basin *P*ALaeoenvironmental research) programme
141 utilized a variety of radiometric dating techniques to try to constrain the ages of different deposits and
142 in doing so create a chronostratigraphic sequence for the basin (Boyer 1999; Boyer et al. 2006; Boyer
143 et al. 2007; Roberts et al. 1999).

144 Çatalhöyük is located to the east of the present course of the Çarşamba River, but the river has been
145 heavily channelized for the last fifty years and so can no longer adjust to changing conditions. It
146 previously debouched from a relatively confined section to the south of Çumra to form an extensive,
147 low-angled fan and in the last century consisted of a single-branched channel which previously passed
148 between the East and West Mounds. The Çarşamba fan has been subject to a variety of
149 interpretations, in part because of its low angle sloped deposits, with its form being described as
150 “more akin to an alluvial floodplain than an alluvial fan environment” (Roberts 1995: 209). Initially,
151 de Meester (1970: 86) described the entry of the river to the basin as deltaic, and it was suggested that
152 the Neolithic soils found upon it were formed under “semi-lacustrine marsh” conditions. The KOPAL
153 project concurred with de Meester’s (1970) assessment of soil formation. Roberts et al. (1999: 624)
154 identified a dark, organic clay deposit that began to form just prior to the foundation of Neolithic
155 Çatalhöyük (*c.* 7400 cal BCE: Bayliss et al. 2015), as representative of a marsh or backswamp
156 deposit. Above it, another dark-grey-brown silt-clay, described as the first truly alluvial deposit
157 (termed the Lower Alluvium) was dated as forming coevally with the occupation of Çatalhöyük (from
158 *c.* 7000 cal BCE), in a seasonally flooding environment, due to its high organic content and lack of
159 coarse sediment (Roberts et al. 1999: 625). The coarser grain size and increased carbonate content in
160 the overlying Upper Alluvium was interpreted as indicative of the catchment area changing between
161 the early and late Holocene (Roberts et al. 1999: 627). In addition, a palaeochannel of the Çarşamba
162 River was identified that contained a variety of coarse-grained sediments and freshwater shells, and,
163 at 42.5 m wide, led the authors to conclude that a large meandering river system rather than a deltaic

164 system was in place on the fan. Later research by Roberts and Rosen (2009) sought to constrain the
165 end of the alluvial flooding phase seen in the Upper Alluvium, suggesting that it may have ceased
166 with the arrival of the 8.2 ka event (i.e. c.6200 cal BCE) identified in Greenland ice cores, which they
167 interpreted regionally as a short, relatively arid and cool interval, and which seemed to have coincided
168 with the abandonment of Çatalhöyük East mound and occupation of the smaller West mound (Roberts
169 and Rosen 2009, 399; Alley and Ágústsdóttir 2005; Gasse 2000).

170 Dryland environments are inherently heterogeneous (Parsons and Abrahams 2009; Müller et al.
171 2013). Care therefore needs to be taken in making extensive spatial and temporal interpretations of
172 landscape reconstruction based on a small number of samples. The review of the evidence from the
173 palaeochannel would indicate that the interpretation of the meandering single channel is not directly
174 dated to the occupation of either mound, as the OSL dates on the fill are much later, in the
175 Chalcolithic (Boyer et al. 2006), while the review of the bioarchaeological evidence by Charles et al.
176 (2014) points to incompatibility of the onsite material with this interpretation. Similarly, there is
177 insufficient chronological detail to allow an interpretation of sedimentation changes in relation to the
178 8.2 ka event that has been suggested as being represented in Turkish speleothem sequences (Göktürk
179 et al 2011:2444) and lake cores (Roberts et al. 2011 and references therein; Roberts et al. 2016:357).
180 Even at the regional scale, the interpretation of aridity is based on a hiatus of sedimentation, which
181 according to Fontugne et al. (1999) lasted for 1,100 to 1,300 years, and potentially as long as 1,500
182 years. Evidence for a short event is thus lacking. In view of these discrepancies driven by sampling as
183 well as analytical constraints, the current project attempts to investigate the landscape through a much
184 higher resolution, intensive sampling programme in which more extensive sediments were sampled in
185 more detail to try to add information into the interpretation, especially the periods immediately
186 preceding and contemporaneous to the occupation of the mounds.

187

188 Materials and methods

189 *Field sampling and sub-sampling*

190 A total of 29 sediment cores were taken in 2007-2013 to provide this higher resolution data (**Figure 1**)
191 by focusing on the immediate environment surrounding the two tells. Previous coring programmes
192 (Boyer et al 2006) had made lower-resolution correlations between relatively few coring locations
193 close to the site with those in larger landscape. The coring programme of 2007-2008 instead focused
194 on an area within 1 km of the site which recent work has suggested would have been more than
195 adequate for supplying the agricultural needs of the site (Bogaard and Isaakidou 2010) and related
196 taskscapes (Charles et al. 2014). The coring locations were distributed in order to ensure
197 representative sampling of potentially varied microenvironments. The purpose of the first two seasons
198 of renewed coring (2007-2008) was to address an immediate inconsistency between the KOPAL

199 wetland model and changing mudbrick compositions. Heavy mudbricks (hundreds required per
200 house) would have been made from raw materials close to the site and borehole locations were
201 constrained accordingly, while also including a few distant control points. As part of larger holistic
202 review of all aspects of clay-based material culture at Çatalhöyük, Doherty (2013) used the sequence
203 of mudbricks as proxies for changing sediment availability immediately around the mound.

204 All cores were extracted with a percussion corer. The cores in 2007 were taken in discontinuous
205 0.5-m sections while in 2008, a system of coring parallel sets of overlapping cores 1-2 m apart was
206 employed to ensure that a continuous sequence was recovered. A total of 21 coring locations of 3 to
207 5 m depth were extracted in 0.5-m sections, described and photographed in the field, wrapped in
208 cellophane and placed in plastic guttering for transportation back to the UK where they were
209 refrigerated prior to analysis. Subsampling for sediment was carried out at 0.05-m intervals on the
210 2007 cores, while sampling was focused on the identified lithological units on 2008 and 2013 cores
211 instead. In the summer of 2013, a further eight coring locations were sampled from an area *c.* 2 km²
212 centred around the Çatalhöyük settlement mounds, using transects that concentrated on areas that had
213 not previously been sampled. At each location a parallel set of overlapping cores were taken 2-3 m
214 apart to a depth of 5 m (8 × 4.50 m from each borehole; the top 0.5 m was discarded due to
215 considerable modern reworking of sediments by agriculture since the Hellenistic-Byzantine period)
216 (Boyer et al. 2006). Following transportation, all cores were then refrigerated to prevent degradation
217 before analysis (Tirlea et al. 2014).

218

219 *Sediment analyses on core lithology*

220 The lithology of the cores was described, in particular the colour, sediment type, and grain size.
221 Munsell soil colour charts were used to precisely log the colour of sediments (Munsell Color
222 Company 1994; Melville and Atkinson 1985). Particle size was noted using a slightly modified
223 Wentworth (1922) description for clastic sediments, and structures within the cores such as transitions
224 and artefacts (e.g. macrofossils) were recorded (Tucker 2011). Any missing or damaged sections were
225 also documented. All cores were analyzed for magnetic susceptibility in a Bartington Instruments
226 MS2 meter, with a continuous loop at 0.02-m intervals. In addition, 443 bulk samples were sub-
227 sampled and measured with a dual frequency sensor type MS2B with a low frequency sensor,
228 following Gale and Hoare's method for measurement at normal sensitivity (1991, 223-229) to provide
229 estimates of volumetric magnetic susceptibility. Loss on ignition of 350 discrete samples was
230 conducted at 550°C and 950°C following Nelson and Sommers (1996) for organic matter content and
231 CaCO₃ equivalent. Approximately 3 grams of sediment were sub-sampled from the same 350 discrete
232 samples tested for LOI for Particle Size Analysis (PSA) using laser diffractometry. Samples were
233 disaggregated and sieved down to 2 mm and weighed. For fractions <2 mm, the methodology

234 followed the HORIBA LA-950 machine protocol, and Gale and Hoare (1991), for the removal of
235 plant organic matter before PSA through wet digestion with hydrogen peroxide prior to
236 disaggregation through the addition of 10 ml of sodium hexametaphosphate 0.1% solution. These
237 observations were then mapped and logged using RockWorks™ v16 software. Individual lithological
238 units were condensed into a series of lithostratigraphic units identifiable across the site, and 2D
239 boreholes were used to visualize the cores. These units were projected onto transects as a fence
240 diagram, showing the locations of the cores relative to one another, allowing changing depositional
241 environments across the site to be identified.

242

243 *Geochemical and isotopic analyses*

244 Core 2013/14 was chosen for more detailed analysis as it produced the most complete and
245 representative sequence of sediments. Subsamples were analyzed to establish the total carbon and
246 nitrogen contents, as well as bulk-sediment carbon-isotope ratio ($\delta^{13}\text{C}$) analysis along with organic
247 carbon-nitrogen (C/N) ratio. This geochemical analysis was carried out to evaluate the source and
248 nature of organic material preserved in the sediments and nature of the vegetation and moisture in the
249 landscape (Chmura et al. 1987; Meyers 1994; Yu et al. 2010), given that previous attempts to extract
250 pollen or diatoms from the sediments had failed. A series of 36 samples were sub-sampled from core
251 2013/14 for total carbon and total nitrogen measurement with sampling resolution ranging from 0.2 m
252 to 0.02 m depending on lithology sampled (more closely sampled across the Dark Clay layer). From
253 this initial sample set 17 levels were selected for more detailed total organic carbon and nitrogen
254 analysis (used for C/N) and subsequently bulk organic $\delta^{13}\text{C}$ analysis. All samples were dried and ball
255 milled before measurements of total carbon and total nitrogen were made using a Carlo Erba CHN
256 Elemental Analyser. The 17 sub-samples from this initial set were then acidified to remove carbonate
257 (CaCO_3), using a modified method from Brodie *et al.* (2011). The samples were then left in a drying
258 cabinet at 40°C for 48 hours before again being milled. Samples were then sent to the BGS
259 laboratories in 5 ml glass bottles with tin lids to prevent plastic contamination, where the total organic
260 carbon, total nitrogen and $\delta^{13}\text{C}$ isotope ratio were measured using a Carlo Erba Elemental CHN
261 Analyser on-line to a Carbon Isotope VG Triple Trap and Optima dual-inlet mass spectrometer.
262 Measurements from the BGS laboratory of the weight ratio of organic carbon to total nitrogen were
263 then used to calculate a final C/N ratio.

264

265 *Dating*

266 Nine samples were selected from the 2013 cores for Accelerator Mass Spectrometer (AMS)
267 radiocarbon dating. Eight samples were from bulk organic material from the fine dark clay

268 sediments, the other sample was from shell fragments (Table I). Radiocarbon dates were
269 carried out by Beta Analytic. Radiocarbon calibration was performed using OxCal 4.2 (Bronk
270 Ramsey 2009) using the IntCal13 calibration curve (Reimer et al. 2013).

271

272 Results

273 Cores taken in 2007 penetrated to a depth of 7.47-8.03 m, while those in 2008 and 2013 were
274 limited to a depth of 5 m (Figure 2). The 2007 and 2008 cores were only extracted every
275 alternate metre, but visual analysis of the intervening sediments was made in the field. The
276 2013 cores were extracted continuously. Based on changes in texture, colour and magnetic
277 susceptibility as well as stratigraphic position, the sedimentary units described have been
278 divided into three groups (Figure 2).

279

280 *Basal Complex*

281 The lowest part of the sequence is made up of marl, and sands with gravel. The sands and
282 gravels tend to be moderately to well sorted, and in units of 0.1 – 0.5 m in thickness. Locally,
283 there are poorly sorted layers containing mixed granules of different lithologies derived from
284 the local limestone bedrock and surrounding sand ridges, as well as from igneous and other
285 bedrocks from further upstream in the Çarşamba catchment (up to small pebbles of 5 mm).
286 Granules and sands are all subrounded to rounded. There was no evidence of structures,
287 although this lack may simply be due to the restricted diameter of the cores. These sands and
288 gravels are typically light brown in colour (2.5Y5/2 or 2.5Y6/2), although locally are darker
289 brown (10YR4/2 or 10YR5/3). There is much lateral variation in texture at equivalent
290 elevations across the landscape. At locations 2007/1-3, 6 and 10, the sands are interbedded
291 with marls and clays which occur in units of 0.05 – 0.5 m in thickness. All locations sampled
292 are capped by a marl layer that varies in thickness from 0.01 m (core 2007/7) to 1.04 m
293 (2013/12). The marl is predominantly light grey (2.5Y1-6/1-2) to white (10YR8/1), and with
294 a clay texture in the lower parts of the section and silty-clay texture towards the top of the
295 complex. Core 2013/12 also contains a laminated Dark Clay layer (see further discussion of
296 the Dark Clay below) 1.1 m below the marl, and another thin Dark Clay layer in between two
297 marl units.

298 Because of its ubiquity, the upper part of this complex was taken as the uppermost
299 appearance of marl in the core, and thus its elevation varies between locations. At its deepest
300 (core 2007/6), the upper boundary is at 6.33 m below the modern ground surface, and at
301 1.65 m at its shallowest (core 2007/4). The upper surface tends to be lower between and
302 immediately to the south of the mounds, but it also undulates in a N-S and E-W direction
303 between cores (Figure 4). In the shorter cores, this complex is absent from 2008/8 and 9 and
304 2013/4.

305 The marls in this complex have a mean organic content of 4.65 ± 0.23 % (SE), CaCO_3
306 content of 45.94 ± 1.71 %, and a mass-specific magnetic susceptibility of $27.99 \pm$
307 $4.28 \times 10^{-8} \text{ m}^3 \text{ kg}^{-1}$. The clastic sediments have a mean organic content of 3.75 ± 0.35 %,
308 CaCO_3 content of 29.18 ± 1.70 % and a mass-specific magnetic susceptibility of $111.87 \pm$
309 $13.31 \times 10^{-8} \text{ m}^3 \text{ kg}^{-1}$.

310 Two dates were obtained from core 2013/12. A level of laminated dark clay (2.5Y2.5/1) at a
311 depth of 3.865-3.88 m produced a date of 27,617-27,011 cal BCE (2σ) on bulk organics. At a
312 depth of 3.82-3.83 m, a date of 44,666-42,555 cal BCE (2σ) on large (up to 20 mm), angular
313 shell fragments was obtained (Table I; Figure 2).

314

315 *Lower Complex*

316 The Lower Complex is dominated by silts, silty clays and clays with some reworked
317 fragments of marl in places (Figure 2). In a number of places (cores 2008/1-3, 2013/17 and
318 18), the marl at the top of the basal complex is directly overlain by a dark grey or black
319 (10YR2/1-4/1, 10YR3/3 or 2.5Y2.5/1) clay (subsequently called Dark Clay). Elsewhere,
320 Dark Clay is absent the lower complex starts with lighter coloured silts and clays (cores
321 2007/5-10, 2008/5, 2013/4, 2013/14-16 and 2013/19: ranging from light greyish brown
322 2.5Y6/2 to grey 10YR5/1), or in the case of core 2007/10, a gravel with silty matrix (2.5Y6/2
323 [light brownish grey]). In core 2007/4 there is a transitional boundary of 0.04 m with the
324 Basal Complex characterised by a mix of marl and the silt. The upper contact of the marl at
325 the top of the Basal Complex was not observed in the other 11 cores. Boundaries are abrupt
326 and smooth or occasionally wavy, suggesting erosional contacts. The dark grey or black clay
327 layer is also found at higher points stratigraphically in the Lower Complex in cores 2007/1-3,
328 2007/7, 2007/8 and 2007/10, 2013/4, 2013/14, 2013/15 and 2013/19, but elsewhere (2013/16)

329 it is absent. The Dark Clay varies from 1-mm thick (2008/3) to between 5-15 mm thick
330 (2007/5 and 9, 2008/1 and 2, 2013/12, 2013/15 and 2013/18) and is made up of coarse clay to
331 fine silt. It often contains small, white CaCO₃ nodules, and has an organic carbon content of
332 2-10 %, 2-26 % CaCO₃ content, and mass-specific magnetic susceptibility of $13-46 \times$
333 $10^{-8} \text{ m}^3 \text{ kg}^{-1}$. The dark and grey clays make up 15 % (by number) of the described units in
334 the lower complex from the 2007-2013 cores.

335 Of the remaining units in the lower complex, 43 % are made up of silty-clays or silts, and a
336 further 11 % of clays. However, there are also a range of sands, granules and gravels,
337 occasionally with silt matrices. For example, in 2013/15, there is a coarse, mixed lithology
338 sand of subangular to angular grains from 1.73-1.94 m in depth. In core 2013/4 there is a
339 fining-upwards sequence from poorly sorted granules (4.64-4.97 m) to coarse sand (4.56-
340 4.64 m) then medium sand with intermixed clays (4.24-4.56 m), and then silty clays or silts
341 (3.7-4.24 m), capped by the dark clay noted above. Colours are dominantly in the range
342 10YR4-6/1-4 (dark grey/grey to light yellowish brown).

343 The mean organic content of the Lower Complex is 6.13 ± 0.20 % (SE), CaCO₃ content is
344 30.90 ± 1.03 %, and a mass-specific magnetic susceptibility is $67.02 \pm 3.78 \times 10^{-8} \text{ m}^3 \text{ kg}^{-1}$.
345 All three variables show a significant difference from the values measured in the Basal
346 Complex ($p < 0.05$).

347 Dates were obtained on bulk organic carbon from sediments from seven samples of the Dark
348 Clay layer. The dates (all 2σ) range from 11,113-10,841 cal BCE to 5,720-5,631 cal BCE
349 (Table I; Figure 2).

350

351 *Upper Complex*

352 The transition to the upper complex also occurs at a wide range of depths. Although it
353 dominantly occurs at 1.5-2.5 m below the modern surface, it varies from 0.74 to 4.07 m. The
354 units are dominantly (51 %) silty-clays or silts, followed by 11 % of clays. Coarse sands are
355 less frequent than in the Lower Complex, but there are still relatively frequently recorded
356 poorly sorted granules (10 %) or sandy silts (15 %). There is a slight tendency for the Upper
357 Complex sediments to be lighter than Lower Complex sediments (more 10YR4-6/1-4 (dark
358 grey/grey to light yellowish brown) and fewer 10YR2-3/1-2 (black to very dark greyish
359 brown). In all locations, the Upper Complex grades up into the modern ploughsoil in the

360 upper 0.5 m or so. The most distinguishing characteristics of this complex are the
361 combination of colour change from the grey to brown expressions of hue and the lower
362 frequency of coarser material (sand and granule fractions).

363 The mean organic content of the Upper Complex is 6.06 ± 0.23 % (SE), CaCO_3 content is
364 30.69 ± 1.07 %, and a mass-specific magnetic susceptibility is $73.28 \pm 2.51 \times 10^{-8} \text{ m}^3 \text{ kg}^{-1}$.
365 None of these variables is significantly different (at $p=0.05$) from the values recorded in the
366 Lower Complex. It was not possible to identify any unit with sufficiently concentrated bulk
367 organics to provide a radiocarbon date.

368

369

370 *Geochemical and isotope analyses*

371 Detailed geochemical and isotope analyses were completed from selected samples across the
372 Basal, Lower and Upper Complexes in core 2013/14 (Figures 3 and 4). The top of the marl
373 marking the top of the Basal Complex is at a depth of 3.3 m. The top of the Lower Complex
374 is represented at 1.87 m by a marked rise in mass-specific magnetic susceptibility from 33.5
375 to $65.0 \times 10^{-8} \text{ m}^3 \text{ kg}^{-1}$. Total nitrogen (TN) values are low (<0.1 %) from 5 m to 3 m (Figure 4).
376 There is a slight increase to 0.17 % at 2.98 m, which is midway through the Dark Clay.
377 Immediately above the Dark Clay, at a depth of 2.92 m, TN peaks at 3.39 %, then declines
378 exponentially to oscillate around 0.6 % from 2.5 – 1.55 m. There is a further peak of 2.45 %
379 at a depth of 1.40 m.

380 Total carbon (TC) is highest in the gravel at the base of the core at 4.9 m (7.06 %), then
381 decreases to plateau at c. 2.5 % in the sands and silts between 4.8 – 3.8 m. In the two marl
382 units (3.54 – 3.82 m and 3.32 – 3.44 m) values peak at around 6 %, with a dip in TC in the
383 interleaved silty-clay layer (3.55 – 3.44 m). Values then decrease over the Dark Clay with
384 only minor peaks in this layer at 2.11 % and 2.27 %. TC then rises to remain around 3.0 % to
385 the surface. Conversely, the C/N ratio is lowest in the Dark Clay with values close to 7. The
386 highest values (15.5 – 15.9) are seen lower in the section in the silty-clay sediment at 4.38 –
387 3.82 m. Above the Dark Clay, the ratio plateaus at c. 10 in silty-clay sediments above 2.7 m.
388 Values of $\delta^{13}\text{C}$ are c. 24 ‰ immediately below the Dark Clay, within which values decrease,
389 reaching a minimum of 26.1 ‰ at 3.0 m. The values steadily increase above the Dark Clay,
390 again reaching about 24 ‰ from 2.7 to 1.4 m in depth.

391

392 Discussion

393 Previous reconstructions of the palaeoenvironment surrounding Çatalhöyük have emphasized
394 the importance of the Dark Clay in the earliest post-lake levels as a continuous, chronological
395 marker, and as a basis for interpreting the landscape as having been dominantly humid
396 (Boyer 1999; Boyer et al. 2006:685; Roberts and Rosen 2009:394). However, the higher
397 resolution coring since 2008 has demonstrated that the Dark Clay is not a single deposit,
398 neither stratigraphically nor chronologically. To have a more refined interpretation of the
399 deposits, it is important first to revisit the nature of lacustrine deposition and drying.

400 Lacustrine sediments preserved in the sequences recorded here are characterized by marl and
401 clay deposits with the coarser sands and gravels diagnostic of fluvial deposition. Core
402 2013/12 shows earlier lake deposition was interrupted in MIS3-2 by local fluvial deposition
403 before returning to lake deposition. The apparently anomalous date of 44,666-42,555 cal
404 BCE (2σ) on shells a few centimetres above the level of laminated dark clay dated to 27,617-
405 27,011 cal BCE (2σ) could be explained by the reworking of older shelly deposits. This
406 interpretation is consistent with the fragmentary nature of the shells, or it may relate to the
407 inclusion of old carbon in the shells, taking the date close to the limit of radiocarbon. This
408 core suggests a series of frequent shifts in fluvial deposition within the Basal Complex,
409 before a return to lacustrine deposition in the upper part of the core (marl deposits from 3.0 –
410 1.52 m: Figure 2c). Although there is no direct date on this final lacustrine deposition, it is
411 likely to relate to the final parts of MIS2. At the latest, the date of 11,113-10,841 cal BCE
412 (2σ) in core 2013/15 suggests the end of lake deposition in this part of the Konya Basin in
413 the later Pleistocene. However, Boyer (1999) provides an OSL date on a sandy loam in a
414 palaeochannel cut into the upper marl at site 95PC2 dated to $13,319 \pm 2050$ BCE by OSL.
415 This date would suggest early fluvial activity in the latest Pleistocene, and a hiatus before
416 deposition of the Dark Clay or other deposits at the base of the Lower Complex.

417 In the 2007-2013 cores, the top of the marl varies from 6.33 m to 1.33 m below the modern
418 ground surface, which corresponds to elevations of 1002.5 – 1005.5 m asl. However,
419 including elevations from cores and sections in Boyer (1999), the range is 999.73 –
420 1006.14 m asl. Thus, local variation in the upper surface of the marl is significant, and what
421 is seen is a highly undulating surface reflecting processes of wind deflation and surface water
422 erosion (e.g. the development of local, low-relief “badlands”) as well as later incision by

423 channels (Figure 5). As the lake retreated aeolian deflation of sediments may also have
424 occurred, caused by strong winds across the basin evidenced by high wave cut notches above
425 the palaeobeaches of the late Pleistocene Lake Konya (Naruse et al. 1997). Without the cover
426 of the palaeolake, this process could have led to quarrying of surface deposits. The magnetic
427 susceptibility of the cores, an indicator of surface erosion (Dearing et al. 1981), is seen to
428 increase slowly in sediments from this point, although sizeable rises in magnetic
429 susceptibility do not occur until later in the sequence. These processes would have been in
430 operation during the time of the hiatus in deposition, noted above, before the formation of the
431 Dark Clays. Thus, the later Pleistocene reflects the development of drier conditions and
432 accelerated local erosion, possibly relating to poor initial colonization of the marl surface by
433 vegetation (see discussion in Fontugne et al. 1999). This local erosion produced a ground
434 surface surrounding the site that would have fallen from east to west, and south to northwest,
435 which would have constrained subsequent river activity as seen in the deposits of the Lower
436 Complex in the area of, or to the west of, the study area (Figure 5; see also Boyer et al. 2006,
437 Figure 7b). Excavations in the immediate vicinity of the east tell have also identified pits dug
438 into the marl and led to interpretations of quarrying the marl near the tell for the production
439 of mudbrick (Roberts et al 2007, Doherty 2013). Doherty (2013) concluded that the observed
440 mudbrick transition resulted directly from a combination of the deep extraction of reddish
441 Pleistocene clay beneath the marl and of large quantities of distal colluvium accumulating in
442 exposed former mudbrick pits. The ability to dig far below the marl and the complete absence
443 of either erosion or of flood deposits in one metre-plus sections of consistently fine-grained
444 colluvium were taken to indicate an absence of seasonal floods. Instead, from a combination
445 of the geomorphological setting, the observed sedimentary structures (or absence of, e.g.
446 levées) and in particular the sediment composition (predominantly clay aggregates), this clay-
447 centric study argued for an alternative alluvial system at Neolithic Çatalhöyük (small
448 channels; very infrequent and low magnitude flooding) (Charles et al, 2014): a re-
449 interpretation that resolves the clay-digging contradictions of the KOPAL model and is also
450 consistent with all aspects of observed clay use at Neolithic Çatalhöyük, and consistent with
451 the interpretation based on the detailed sedimentological analysis herein.

452

453 The Lower Complex thus began to deposit and infill this undulating surface. Where the Dark
454 Clay is present, most samples predate the occupation of the East Mound (which starts
455 between 7150-7100 cal BCE according to Bayliss et al. 2015; Figure 6). However, there are

456 also late pockets of development of the Dark Clay in some places, as suggested by the sample
457 from 2013/4. The Dark Clay in 2013/4 is contemporary with dates from the West Mound
458 (5,720-5,631 cal BCE compared to c.6150 to 5,500 cal BCE based on dates in Higham et al.
459 (2007) (Figure 5). All of the dating evidence suggests that the Dark Clay is both spatially and
460 temporally discontinuous, refining previous interpretations of a marshy environment in all of
461 the low points of the landscape solely in the Early Holocene (Boyer 1999). Boyer et al
462 (2006:683) suggests the ubiquity of this dark clay directly overlying the marl although this
463 interpretation is contradicted by their Figure 7b, in which it only occurs in some of the lower
464 points in the landscape. Furthermore, Boyer et al (2006: 685) suggests that deposition of the
465 dark organic clay is from 7850-7450 cal BCE (1 sigma), however they were only able to date
466 the material directly at Kızıl höyük and Avrathanı höyük, which are approximately 6-8 km to
467 the northeast and northwest, respectively, of Çatalhöyük. Five of our dates belong to the
468 period 11113 – 9218 cal BCE (2σ), so predate the “broadly contemporaneous deposition”
469 (Boyer et al. 2006: 685) suggested based on correlation. One date of 8223 – 7948 cal BCE
470 (2013/19 to the north of Çatalhöyük) overlaps the dates of Boyer et al. at 2σ (their dates
471 correspond to 8198-7083 cal BCE when calibrated to 2σ using OxCal 4.2), but our dates
472 from both much earlier and much later suggest that the facies is more likely to relate to local
473 conditions rather than regional ones.

474 The Lower Complex is a mix of both coarse and fine sediments – including the Dark Clay –
475 with significant lateral and vertical variability. This pattern of facies is consistent with
476 deposition from an anabranching river system. As there is a tendency for there to be fewer
477 Dark Clays and fewer coarser deposits at higher positions in the sequence, there is a
478 suggestion that there may have been a shift from more humid to dryland anabranching
479 conditions, following the definitions of Nanson and Knighton (1996) and North et al. (2007)
480 (Figure 7). Dryland anabranching rivers have variable morphology and sedimentary
481 behaviour, but one such sub-system, the mud-dominated system, seems to fit the current data
482 for the Lower Complex very well. Under this model (Type 1c of Nanson and Knighton
483 1996), the mud (silt and clay)-dominated system is characterized by a low-gradient
484 floodplain, which has a low rate of aggradation, and a very slight difference between the
485 nature of the deposits in channel and on the floodplain thus not presenting the classic fluvial
486 indicators such as sand-filled channel bodies, lag conglomerates, current ripples and dunes,
487 and fining-up units (North et al. 2007, 930, their Table 2). As a dryland anabranching
488 system, new channels would form via obstruction, which North et al. (2007: 930) define as a

489 much more gradual process than channel change by avulsion. While avulsion is an energetic
490 and rapid process, that requires the channel to cut through solid, vegetation-strengthened
491 channel embankments in a humid river system, in a dryland system, new channels face less
492 resistance to avulsion and are therefore formed more “gradually and incrementally” (North et
493 al. 2007: 930). The frequent sands and silts present in the Lower Complex (cores 2007/1, 2,
494 3, 6, 7, 10; 2008/8&9, 10&11; and 2013/14 and 15), would indicate the distribution of these
495 anabranching palaeochannels between the undulations in the marl as opposed to episodic
496 fluctuation of flow. This interpretation is in contrast to the laterally continuous and extensive
497 deposition of “backswamp clay” (Boyer 1999; Boyer et al 2006: 685; Roberts and Rosen
498 2009:394). Dating evidence suggests that the Lower Complex brackets the occupation of East
499 Mound and at least some of the West Mound (Figure 6). It is possible that the late Dark Clay
500 in core 2013/4 formed as a result of a local hydrological blockage as the development of the
501 West Mound started to cause diversion of pre-existing channels. Most deposition of the
502 Lower Complex is in the southern and western parts of the study area, suggesting a
503 progressive infilling of the landscape (Figure 5).

504 Bi-plots of $\delta^{13}\text{C}$ against C/N ratios in core 2013/14 relative to measured values for freshwater
505 algae, C_3 and C_4 plants and various soils (Figure 8) can be used to interpret potential sources
506 of organic material (Meyers 1997, Yu et al. 2010). In comparisons with the measured soil
507 samples from Yu et al. (2010), samples within the silt unit underlying the Dark Clay (>3.1 m
508 depth) fall within the riverbank soil range, and samples above the Dark Clay (<2.76 m) are
509 also most closely clustered around the lower range of riverbank soil (Figure 8). The silty-clay
510 unit immediately above the Dark Clay (2.92 – 2.76 m) has a broad range of values close to, or
511 within the range of riverbank soils. Samples from the Dark Clay have low $\delta^{13}\text{C}$ and C/N
512 ratios, clustering close to and within the freshwater algal field indicating significant
513 proportions of freshwater algal organic material. The sediments in core 2013/14 both
514 underneath and immediately above the Dark Clay suggest drier conditions than during the
515 Dark Clay. Despite the low organic matter contents, the Dark Clay is probably representative
516 of localized marshy or channel cutoff conditions with periods of standing water, as reflected
517 by the high algal content. Thus, the inherited, undulating environment provided areas that
518 were relatively stable and (at least seasonally) dry during the initial occupation of
519 Çatalhöyük. Indeed, while there is substantial evidence for the presence of wetlands in the
520 archaeozoological and archaeobotanical record at Çatalhöyük (Atalay and Hastorf, 2006),
521 organic matter content in the sedimentological record is quite low, there are no buried peat

522 deposits, and pollen preservation, which is common in anoxic and acidic wetland deposits
523 (Moore et al. 1991), is largely absent here. Wetlands present in the vicinity of Çatalhöyük are
524 likely to have been limited, marked by flowing water with limited standing water, and
525 seasonally desiccated which may help explain the low organic readings in the dark clay
526 layers. These wetter areas are likely to have been more common to the west, with drier
527 conditions more dominant to the east of the site, based on the palaeotopography.

528 Nitrogen levels rise significantly immediately following the Dark Clay in Core 2013/14
529 (Figure 4). A possible explanation is that regular deflation can cause increases in nutrient
530 concentration, and so increase total nitrogen concentration (Scholz et al. 2002). Study of soils
531 has shown that drying and rewetting causes increased nitrogen levels due to microbial death,
532 causing nitrate and ammonia to form, and although some of this is flushed with rewetting, a
533 proportion remains fixed in soil (van Gestel et al. 1991). This response has been seen as an
534 increased concentration in nitrogen in the floodwaters from ephemeral basins following
535 desiccation (Scholz et al. 2002). Alternatively, nitrogen from a geological origin could
536 indicate a changing river input, which would be supported by the fact that the increase in
537 nitrogen is accompanied by a decrease in total carbon content in the core. Contrary to the
538 suggestion of Boyer et al. (2006) that the Çarşamba did not break through the sand spit at
539 Çumra formerly bordering Palaeolake Konya until about 7,000 cal BCE, the presence of
540 sandy deposits in the Lower Complex here suggests that the breach did in fact occur much
541 earlier. This interpretation is consistent with the dated sandy loam in Boyer's (1999) section
542 95PC2, which is part of a channel fill cut into marl dated to $13,319 \pm 2050$ BCE by OSL.
543 The nitrogen data are thus also consistent with the interpretation of increasing desiccation in
544 the fluvial environment. Further to this it is also possible that anthropogenic additions in the
545 form of penning, manuring or middening coming from the settlement could also have
546 impacted upon the nitrogen levels from the time of occupation (Vaiglova et al 2014, Fraser et
547 al 2011), although caution is required with this interpretation until more data are available
548 from cores elsewhere in the landscape.

549 The Upper Complex is more difficult to date, as none of the 2007-2013 cores contain
550 dateable material. There is some evidence for a change in style of deposition, with more fine
551 material than in the Lower Complex, although there continues to be some lateral variability
552 reflecting the palaeotopography. Boyer (1999) suggests that the onset of this phase can be
553 estimated from an OSL date in section 95PC1, of 3548 ± 1337 BCE. Thus, it postdates the
554 occupations of both mounds at Çatalhöyük.

555 In summary, we propose that the palaeoenvironmental evolution of the area surrounding the
556 Çatalhöyük tells, up to the period of their occupation, can be illustrated as four phases (Figure
557 9). Following the retreat of Palaeolake Konya towards the end of the Pleistocene, Phase 1
558 consists of dominant erosion due to wind and water that created an undulating surface of
559 marl. The topography of the study area would have varied by about 7 m by the end of this
560 phase. Sands and gravel provide possible evidence of early fluvial activity, although near-
561 shore deltaic deposits cannot be excluded because of the lack of observed sedimentary
562 structures. Within the sequences demonstrated by the 2007-2013 cores, Phase 1 is the hiatus
563 between the top of the Basal Complex and the start of the Lower Complex. Phase 2 occurs in
564 the latest Pleistocene and early Holocene, and indicates increased wetness, probably
565 characteristic of a humid anabranching channel system, in which there are localized pockets
566 of wetter conditions, relating to local hollows or cutoffs in the channel system. The
567 undulating topography is starting to infill during this phase. In Phase 3a, this infilling
568 continues, producing a flatter surface, and there are fewer pockets being occupied by wetter
569 conditions. The fluvial régime shifts from humid to dryland anabranching conditions, which
570 are more concentrated in the west of the study area. The earliest period of occupation of the
571 East Mound coincides with this phase. This interpretation is more consistent with the
572 archaeological evidence from the site for a mosaic of both dry and wet conditions. Phase 3b
573 coincides with the shift of occupation to the West Mound, when there is evidence for a
574 localized wetter area to the southeast of the mound, but otherwise a continuation of the
575 dryland anabranching system. Phases 2 and 3 represent deposition in the Lower Complex.
576 Finally, Phase 4 (not illustrated) – representing deposition in the Upper Complex – shows a
577 shift to the pre-modern style of fluvial environment, modified by channelization as
578 demonstrated by Boyer (1999) and Boyer et al. (2006). Finally, to clarify the terminology
579 developed here, the Basal Complex is defined as the late Pleistocene deposition in fluvial and
580 lacustrine environments, ending in a widespread erosional phase in the basin. The Lower
581 Complex commences in the final part of the Pleistocene and is broadly parallel to the Lower
582 Alluvium in previous studies. The Upper Complex is parallel to the Upper Alluvium. In all
583 cases, there is significant vertical and lateral variability in facies, hence our preference for the
584 term “Complex”.

585

586

587 Conclusions

588 Contrary to the palaeoenvironmental reconstruction based on the geoarchaeological work that
589 situated Çatalhöyük within a palaeolandscape dominated by wet conditions (Roberts 1996,
590 1999; Boyer 1999, Boyer et al. 2006), the high-resolution coring carried out since 2007 has
591 been able to demonstrate that the landscape was highly variable and has shown evidence of
592 increasingly dry conditions from the early Holocene. While earlier work identified the
593 general sedimentary sequence, the intensive coring programme (adding a further 29 coring
594 locations to the previous nine) and subsequent 3D modelling has identified important
595 localised variability of the alluvial landscape, particularly around the site. Moreover, the
596 inclusion of the geochemical and isotope analysis and further dating of the sediments has
597 enhanced our understanding of the fluvial regime and the degree of wetness around the site
598 during occupation of the Eastern Tell occupied during the Neolithic.

599

600 This new evidence forces us to review the established landscape model and related
601 interpretations of Neolithic land use at the site. The earlier idea that a large single channel
602 flowed past the site in a high-energy meandering river system (Roberts and Rosen 2009:395-
603 6, 399, and their Figure 2b; Roberts et al 1996: 39 but *cf* *ibid* p, 37; Boyer 1999: 97, and his
604 figure 4.19 but note he firmly places the date as later in the Calcolithic) has had a lasting
605 impact on the interpretation of the site especially on discussions of early farming practice.
606 Rosen and Roberts (2005) argued that the territory around the site was so heavily affected by
607 seasonal flooding that areas of viable agriculture were available only in the highlands at a
608 distance of 12 km from the site (and see Roberts et al. 1996, 1999; Roberts and Rosen 2009;
609 Rosen and Roberts 2005; Fairbairn et al. 2002; Fairbairn 2005). We argue that the river
610 system contemporaneous with the settlement was anabranching which means that the large-
611 scale overbank flooding envisaged in previous analyses (Boyer et al. 2006) is of limited
612 application for the archaeological interpretations of the occupation of Çatalhöyük and human
613 responses to changing environmental circumstances. This interpretation is also consistent
614 with the lack of levées observed (Roberts, *pers. comm.*, Roberts et al. 1997:39), which would
615 provide evidence of such overbank flooding, even on the palaeochannel that postdates the
616 settlement. Thus, the Neolithic landscape is likely to be one of mosaics both in space and in
617 time, which is reflected in the variability of the sedimentary sequence. Bogaard et al. (2014)
618 used isotopic work on both faunal and botanical evidence that has proposed relatively local,

619 small-scale herding and farming took place during the Neolithic; such a model is consistent
620 with our new interpretation of the landscape contemporary with the occupation of the site.

621 This study has shown that while rigorous, the previous palaeoenvironmental model based on
622 a limited number of data points near the site coupled with assumptions derived from the
623 investigation of widely distributed (spatially and chronologically) coring locations failed to
624 pick up the variability of the dynamic landscape which would have presented itself to the
625 Neolithic inhabitants. Furthermore, the data produced a model of Neolithic *taskscales* which
626 now requires revision. There is a broader implication for geoarchaeological practice, in that
627 sampling needs to reflect the nature of the environment being studied and its variability.
628 Where there is significant heterogeneity as here, and in dryland environments in general,
629 palaeoenvironmental reconstruction needs to be carried out using as high spatial and temporal
630 resolutions as is possible.

631

632

633 Acknowledgments

634 We thank Ian Hodder for the opportunity to participate in the Çatalhöyük Research Project.
635 Funding for this project was provided by the Templeton Foundation (grant no., 13463, PI
636 Hodder) and the Çatalhöyük Research Project. We are extremely grateful to Amy Bogaard,
637 Mike Charles, and Liz Stroud for field assistance; to Hannah Russ and Harriet White, Bradley
638 Brandt and Sophia Lapidaru who all ran samples at the University of Sheffield; and to Alison
639 George, Frank Davies and Katheryn Melvin who assisted with samples at Durham
640 University. We are also very grateful to Neil Roberts for discussions about the
641 palaeoenvironmental interpretations of the site, and for access to past observations made
642 during the KOPAL projects. We would like to thank Glynis Jones, Caroline Jackson and
643 Matthew Fitzjohn for comments on earlier drafts. We would like to thank the editors and two
644 anonymous reviewers who commented upon and improved this manuscript. All
645 interpretations contained herein remain the responsibility of the authors.

646

647 **References**

- 648 Alley, R.B., Ágústsdóttir, A.M., 2005. The 8k event: cause and consequence of a major Holocene
649 abrupt climate change. *Quaternary Science Reviews*. 24, 1123–1149.
- 650 Atalay, S., Hastorf, C. A., 2006. Food, meals, and daily activities: food habitus at Neolithic
651 Çatalhöyük. *American Antiquity*. 71 (2), 283–319.
- 652 Bayliss, A., Brock, F., Farid, S., Hodder, I., Southon, J., Taylor, R.E., 2015. Getting to the Bottom of
653 It All: A Bayesian Approach to Dating the Start of Çatalhöyük. *Journal of World Prehistory*. 28, 1–26.
- 654 Bogaard, A., Isaakidou, V., 2010. Community size, ideology and the nature of early farming
655 landscapes in Western Asia and Europe, in: Finlayson, B., Warren, G. (eds) *Landscapes in Transition*.
656 Oxbow Books, Oxford. pp. 192–207.
- 657 Bogaard, A., Henton, E., Evans, J.A., Twiss, K.C., Charles, M.P., Vaiglova, P., Russell, N., 2014.
658 Locating land use at Neolithic Çatalhöyük, Turkey: The implications of ⁸⁷Sr/ ⁸⁶Sr signatures in plants
659 and sheep tooth sequences. *Archaeometry*. 56(5), 860–877.
- 660 Bottema, S., Woldring, H., 1984. Late Quaternary vegetation and climate of south-western Turkey.
661 *Paleohistoria*. 26, 123–149.
- 662 Boyer, P., 1999. A geoarchaeological approach to Late Quaternary environmental change in South
663 Central Turkey. Unpublished Ph.D. thesis, Loughborough University.
- 664 Boyer, P., Roberts, N., Baird, D., 2006. Holocene Environment and Settlement on the Çarşamba
665 Alluvial fan, South-Central Turkey: Integrating Geoarchaeology and Archaeological Field Survey.
666 *Geoarchaeology*. 21(7), 675–698.
- 667 Boyer, P., Roberts, N., Merrick, J., 2007. KOPAL excavations at Çatalhöyük 1996–2001. In I.
668 Hodder (Ed.), *Excavating Çatalhöyük: Reports from the 1995–1999 seasons*. Çatalhöyük Project vol.
669 3, pp. 551–570. Cambridge: McDonald Institute for Archaeological Research; London: British
670 Institute of Archaeology at Ankara.
- 671 Brodie, C.R., Leng, M.J., Casford, J.S.L., Kendrick, C.P., Lloyd, J.M., Yongqiang, Z., Bird, M., 2011.
672 Evidence for bias in C and N concentrations and $\delta^{13}\text{C}$ composition of terrestrial and aquatic organic
673 materials due to pre-analysis acid preparation methods. *Chemical Geology*. 282, 67–83.
- 674 Bronk Ramsey, C., 2009. Bayesian analysis of radiocarbon dates. *Radiocarbon*, 51(1), 337–360.
- 675 Cessford, C. 2001. A new dating sequence for Çatalhöyük, *Antiquity*. 75:717–725.
- 676 Charles, M., Doherty, C., Asouti, E., Bogaard, A., Henton, E., Larsen, C.S., Ruff, C.B., Ryan, P.,
677 Sadvari, J.W., Twiss, K.C., 2014. Landscape and taskscape at Çatalhöyük: An integrated perspective,

678 in: Hodder, I., (Ed.) Integrating Çatalhöyük: Themes from the 2000–2008 seasons. Cotsen Institute of
679 Archaeology, Los Angeles, pp. 71–90.

680 Chmura, G.L., Aharon, P., Socki, R.A., Abernethy, R., 1987. An inventory of ¹³C abundances in
681 coastal wetlands of Louisiana, USA: vegetation and sediments. *Oecologia* 74, 264–271.

682 de Meester, T., 1970. Soils of the Great Konya Basin, Turkey. Wageningen: Centre for Agricultural
683 Publishing and Documentation.

684 de Ridder, N. A., 1965. Sediments of the Konya basin, central Anatolia, Turkey. *Palaeogeography,*
685 *Palaeoclimatology, Palaeoecology.* 1, 225–254.

686 Dearing, J. A., Elnor, J. K., Haphey-Wood, C. M., 1981. Recent sediment flux and erosional processes
687 in a Welsh upland lake-catchment based on magnetic susceptibility measurements. *Quaternary*
688 *Research.* 16(3), 356–372.

689 Doherty, C., Charles, M., Bogaard A., 2007. Preliminary sediment coring to clarify ‘clay’ sources and
690 potential land-use around Çatalhöyük. *Çatalhöyük Archive Report*, 382–390.

691 http://www.catalhoyuk.com/archive_reports/2007 (last accessed 19.10.16)

692 Doherty, C., Charles, M., Bogaard A., 2008. Landscape coring. *Çatalhöyük Archive Report*, 263–272.
693 http://www.catalhoyuk.com/archive_reports/2008 (last accessed 19.10.16)

694 Doherty, C., 2013. Sourcing Çatalhöyük’s clays. In I. Hodder (Ed.), *Substantive Technologies at Catalhöyük: Reports*
695 *from the 2000–2008 seasons.* Los Angeles: Cotsen Institute of Archaeology Press, pp.331-63.

696 Doherty, C., 2013. Sourcing Çatalhöyük’s clays. in: I. Hodder (ed.), *Substantive technologies at*
697 *Çatalhöyük: Reports from the 2000–2008 Seasons: (Çatalhöyük Research Project Volume 9).*
698 London: British Institute at Ankara; Los Angeles, Cotsen Institute of Archaeological Press, 51-66.

699 Fairbairn, A., 2005. A history of agricultural production at Çatalhöyük East, Turkey, *World*
700 *Archaeology.* 37, 197–210.

701 Fairbairn, A. S., Asouti, E., Near, J., Martinoli, D., 2002. Macro-botanical evidence for plant use at
702 Neolithic Çatalhöyük, south-central Anatolia, Turkey. *Vegetation History and Archaeobotany.* 11,
703 41–54.

704 Fontugne, M., Kuzucuoğlu, C., Karabiyikoğlu, M., Hatté, C., Pastre, J.-F., 1999. From Pleniglacial to
705 Holocene: a ¹⁴C chronostratigraphy of environmental changes in the Konya Plain, Turkey. *Quaternary*
706 *Science Reviews.* 18, 573–591.

707 Fraser, R.A., Bogaard, A., Heaton, T., Charles, M., Jones, G., Christensen, B.T., Halstead, P.,
708 Merbach, I., Poulton, P.R., Sparkes, D. and Styring, A.K., 2011. Manuring and stable nitrogen isotope

709 ratios in cereals and pulses: towards a new archaeobotanical approach to the inference of land use and
710 dietary practices. *Journal of Archaeological Science*, 38(10), pp.2790-2804.

711 Gale, S., Hoare, P. G., 1991. *Quaternary sediments: Petrographic methods for the study of unlithified*
712 *rocks*. Belhaven Press; Halsted Press, London, New York, pp. 223–229.

713 Gasse, F., 2000. Hydrological changes in the African tropics since the Last Glacial Maximum.
714 *Quaternary Science Reviews*. 19, 189–211.

715 Göktürk, O.M., Fleitmann, D., Badertscher, S., Cheng, H., Edwards, R.L., Leuenberger, M.,
716 Fankhauser, A., Tüysüz, O. and Kramers, J., 2011. Climate on the southern Black Sea coast during the
717 Holocene: implications from the Sofular Cave record. *Quaternary Science Reviews*, 30(19), pp.2433-
718 2445.

719 Higham, T. F. G., Bronk Ramsey, C., Brock, F., Baker, D., Ditchfield, P., 2007. Radiocarbon dates
720 from the Oxford AMS system: *Archaeometry Datelist 32*. *Archaeometry* 49: S1–S60. Oxford
721 University, Research Laboratory for Archaeology and the History of Art, Oxford.

722 Kuzucuoğlu, C., Bertaux, J., Black, S., Deneffe, M., Fontugne, M., Karabiyikoğlu, M., Kashima, K.,
723 Limondin-Lozouet, N., Mouralis, D., Orth, P., 1999. Reconstruction of climatic changes during the
724 Late Pleistocene, based on sediment records from the Konya Basin (Central Anatolia, Turkey).
725 *Geological Journal*. 34, 175–198.

726 Melville, M. D., Atkinson, G., 1985. Soil colour: its measurement and its designation in models of
727 uniform colour space. *Journal of Soil Science*. 36(4), 495–512.

728 Meyers, P.A., 1994. Preservation of elemental and isotopic source identification of sedimentary
729 organic matter. *Chemical Geology*. 114, 289–302.

730 Meyers, P.A., 1997. Organic geochemical proxies of paleoceanographic, paleolimnologic, and
731 paleoclimatic processes. *Organic Geochemistry*. 27(5/6), 213–250.

732 Moore, P.D., Webb, J.A. and Collinson, M.E., 1991. *Pollen analysis*. Blackwell Scientific
733 Publications, Oxford.

734 Müller, E.N., Wainwright, J., Parsons A.J., Turnbull, L. (Eds) 2013. *Patterns of Land-Degradation in*
735 *Drylands: Understanding Self-Organized Ecogeomorphic Systems*. Springer, Dordrecht.

736 Munsell Colour Company, 1994. *Munsell Soil Color Charts*. Macbeth Division of Kollmorgen
737 Instruments Corporation, New Windsor, NY, 12553.

738 Nanson, G. C., Knighton, A. D., 1996. Anabranching rivers: their cause, character and classification.
739 *Earth surface processes and landforms*. 21(3), 217–239.

740 Naruse, T., Kitagawa, H., Matsubara, H., 1997. Lake level changes and development of alluvial fans
741 in Lake Tuz and the Konya Basin during the last 24,000 years on the Anatolian Plateau, Turkey.
742 *Japan Review*. 8, 173–192.

743 Nelson, D.W., Sommers, L.E., 1996. Total Carbon, Organic Carbon and Organic Matter, in: Sparks,
744 D.L., Page, A.L., Helmke, P.A. (Eds.), *Methods of Soil Analysis: Book series No. 5, Part 3 Chemical*
745 *Methods*. Soil Science Society of America, Madison, pp. 961–1010.

746 North, C.P., Nanson, G.C., Fagan, S.D., 2007. Recognition of the Sedimentary Architecture of
747 Dryland Anabranching (Anastomosing) Rivers. *Journal of Sedimentary Research*. 77 (11), 925–938.

748 Parsons, A.J., Abrahams A.D. (Eds) 2009 *Geomorphology of Desert Environments*, 2nd edition,
749 Springer, Berlin.

750 Reimer, P. J., Bard, E., Bayliss, A., Warren Beck, J., Blackwell, P.G., Bronk Ramsey, C., Buck, C.E.,
751 Cheng, H., Lawrence Edwards, R., Friedrich, M., Grootes, P.M., Guilderson, T.P., Haflidason, H.,
752 Hajdas, I., Hatté, C., Heaton, T.J., Hoffmann, D.L., Hogg, A.G., Hughen, K.A., Felix Kaiser, K.,
753 Kromer, B., Manning, S.W., Niu, M., Reimer, R.W., Richards, D.A., Marian Scott, E., Southon, J.R.,
754 Staff, R.A., Turney, C.S.M., van der Plicht, J., 2013. IntCal13 and Marine13 radiocarbon age
755 calibration curves 0–50,000 years cal bp. *Radiocarbon*. 55, 1869–1887.

756 Roberts, N., 1991. Late Quaternary geomorphological change and the origins of agriculture in south
757 central Turkey. *Geoarchaeology*. 6(1), 1-26.

758 Roberts, N., 1995. Climatic forcing of alluvial-fan regimes during the Late Quaternary in the Konya
759 Basin, south central Turkey, in: Woodward, J., Lewin, J., Macklin, M. (Eds.), *Mediterranean*
760 *Quaternary River environments*. A.A. Balkema, Rotterdam, pp. 207–217.

761 Roberts, N., Rosen, A., 2009. Diversity and Complexity in Early Farming Communities of Southwest
762 Asia: New Insights into the Economic and Environmental Basis of Neolithic Çatalhöyük. *Current*
763 *Anthropology*. 50(3), 393–402.

764 Roberts, N., Boyer, P., Parish, R., 1996. Preliminary results of geoarcheological investigations at
765 Çatalhöyük. In I. Hodder (Ed.), *On the surface: Çatalhöyük 1993–1995. Çatalhöyük Research Project*
766 *Volume 1*; British Institute for Archaeology at Ankara Monograph 22, pp.19–40. Cambridge:
767 McDonald Institute for Archaeological Research.

768 Roberts, N., Black, S., Boyer, P., Eastwood, W.J., Griffiths, H.I., Lamb, H.F., Leng, M.J., Parish, R.,
769 Reed, J.M., Twigg, D., Yiğitbaşıoğlu, H., 1999. Chronology and stratigraphy of Late Quaternary
770 sediments in the Konya Basin, Turkey: Results from the KOPAL project. *Quaternary Science*
771 *Reviews*. 18, 611–630.

- 772 Roberts, N., Boyer, P., Merrick, J., 2007. The KOPAL On-site and Off-site Excavations and
773 Sampling. In I. Hodder (Ed.) Excavating Çatalhöyük: South, North and KOPAL Area reports from the
774 1995-99 seasons. Çatalhöyük Research Project Volume 3; British Institute for Archaeology at Ankara
775 Monograph 37, pp.553-573.
- 776 Roberts, N., Eastwood, W.J., Kuzucuoğlu, C., Fiorentino, G. and Caracuta, V., 2011. Climatic,
777 vegetation and cultural change in the eastern Mediterranean during the mid-Holocene environmental
778 transition. *The Holocene*, 21(1), pp.147-162.
- 779 Roberts, N., Allcock, S.L., Arnaud, F., Dean, J.R., Eastwood, W.J., Jones, M.D., Leng, M.J.,
780 Metcalfe, S.E., Malet, E., Woodbridge, J. and Yiğitbaşıoğlu, H., 2016. A tale of two lakes: a multi-
781 proxy comparison of Lateglacial and Holocene environmental change in Cappadocia, Turkey. *Journal*
782 *of Quaternary Science*, 31(4), pp.348-362.
- 783 Rosen, A., Roberts, N., 2005. The nature of Çatalhöyük, people and their changing environments in
784 the Konya Plain. In I. Hodder (Ed.), Çatalhöyük perspectives: Reports from the 1995–1999 seasons.
785 Çatalhöyük Research Project Volume 6; British Institute for Archaeology at Ankara Monograph 40,
786 pp. 39–53. Cambridge: McDonald Institute for Archaeological Research.
- 787 Russell, N., Martin, L., 2005. The Çatalhöyük mammal remains, in: Hodder, I. (Ed.) Inhabiting
788 Çatalhöyük: Reports from the 1995-1999 seasons. The McDonald Institute for Archaeological
789 Research / British Institute of Archaeology at Ankara Monograph, pp. 33–98.
- 790 Scholz, O., Gawne, B. E. N., Ebner, B., Ellis, I., 2002. The effects of drying and re-flooding on
791 nutrient availability in ephemeral deflation basin lakes in western New South Wales, Australia. *River*
792 *Research and Applications*. 18(2), 185–196.
- 793 Sherratt, A. 1980. Water, soil and seasonality in early cereal cultivation. *World Archaeology*. 11,
794 313–330.
- 795 Tirlea, D., Beaudoin, A.B., Vinebrooke, R.D., 2014. Freeze-dried is as good as frozen: Evaluation of
796 differential preservation of pollen grains in stored lake sediments. *Review of Palaeobotany and*
797 *Palynology*. 215, 46–56.
- 798 Tucker, M.E. 2011. *Sedimentary Rocks in the Field: A Practical Guide*. 4th edition. Wiley-Blackwell,
799 Chichester.
- 800 Vaiglova, P., Snoeck, C., Nitsch, E., Bogaard, A. and Lee-Thorp, J., 2014. Impact of contamination
801 and pre-treatment on stable carbon and nitrogen isotopic composition of charred plant remains. *Rapid*
802 *Communications in Mass Spectrometry*, 28(23), pp.2497-2510.

803 van Gestel, M., Ladd, J.N., Amato, M., 1991. Carbon and Nitrogen mineralisation from two soils of
804 contrasting texture and microaggregate stability: Influence of sequential fumigation, drying and
805 storage. *Soil Biology Biochemistry*. 23(4), 313–322.

806 Wentworth, C.K., 1922. A scale of grade and class terms for clastic sediments. *The Journal of*
807 *Geology*. 30(5), 377–392.

808 Woldring H, Bottema S. 2003. The vegetation history of East-Central Anatolia in relation to
809 archaeology: the Eski Acıgo 1 pollen evidence compared with the Near Eastern environment.
810 *Palaeohistoria* 43/ 44: 1–34.

811 Yu, F., Zong, Y., Lloyd, J.M., Huang, G., Leng, M.J., Kendrick, C., Lamb, A.L., Yim, W.W.-S.,
812 2010. Variability of bulk organic $\delta^{13}\text{C}$ and C/N in the Pearl River delta and estuary, southern China
813 and its indication for sources of the organic carbon. *Estuarine, Coastal and Shelf Science* 87, 618–630.
814 DOI: 10.1016/j.ecss.2010.02.018.

815

816

Pre-publication Copy

817 List of Tables

818 Table I Radiocarbon-dated materials from the cores sampled in 2013. Radiocarbon
819 calibration was performed using OxCal 4.2 (Bronk Ramsey 2009) using the IntCal13
820 calibration curve (Reimer et al. 2013).

821

822

Pre-publication copy

823 List of Figures

824 Figure 1 Location of the study site: a. general setting of Çatalhöyük and the transition
825 between uplands and the Konya basing; and b. map of coring locations from this and previous
826 studies in relation to the two tells at the site. The other lines are irrigation features and the
827 location of the modern river where not directly channelized

828 Figure 2 Lithostratigraphic logs of the cores sampled in this study: a. cores from 2007; b.
829 cores from 2008; and c. cores from 2013. Stratigraphic interpretations are shown in relation
830 to the Basal (BC), Lower (LC) and Upper (UC) Complexes as discussed in the text.

831 Figure 3 Photographic log of core 2013/14 showing the relationship between lithological and
832 stratigraphic interpretations.

833 Figure 4 Results of isotopic and geochemical analyses of core 2013/14: showing the
834 lithostratigraphic log and corresponding changes in properties. The legend for the log is the
835 same as in Figure 2.

836 Figure 5 Interpreted stratigraphic fence diagram showing the spatial patterns of the
837 stratigraphic changes in relation to the two mounds. Gaps in the fences relate to locations
838 where archaeological material dominated the stratigraphy, from the samples in previous
839 studies. Fence diagram produced by interpolation using Rockworks 16.

840 Figure 6 Radiocarbon dates of sediment from this and previous studies. The date ranges on
841 the bottom of the diagram relate to the early archaeological occupation of the East Mound
842 (Bayliss et al., 2015) and of the West Mound (Higham et al. 2007). Radiocarbon calibration
843 was performed using OxCal 4.2 (Bronk Ramsey 2009) using the IntCal13 calibration curve
844 (Reimer et al. 2013).

845 Figure 7 Examples of humid (A) and dryland (B) anabranching channels redrawn from
846 Nanson and Knighton (1996) and from North et al. 2007.

847 Figure 8 Graph showing the relationship of the C/N and $\delta^{13}\text{C}$ values in relation to known
848 environments based on the studies of Meyers (1997) and Yu et al. (2010).

849 Figure 9 Schematics of the landscape-development phases: a. Phase 1 (later Pleistocene, with
850 localized erosion producing low-relief “badland” topography); b. Phase 2 (latest Pleistocene
851 and early Holocene with the formation of a humid anabranching channel); c. Phase 3a (shift
852 to dryland anabranching channel and ultimately occupation of the East Mound); and d. Phase

853 3b (continuation of dryland anabranching channel and shift to occupation of the West
854 Mound).

Pre-publication copy

Table I Radiocarbon-dated materials from the cores sampled in 2013. Radiocarbon calibration was performed using OxCal 4.2 (Bronk Ramsey, 2009) using the IntCal13 calibration curve (Reimer *et al.*, 2013).

Sample core – depth [m]	Material dated	Uncalibrated AMS age years bp	Calibrated age cal BCE 2σ	Laboratory code	Stratigraphic context*	Notes
2013/4 3.43-3.44	Bulk organics	6770 ± 30	5720 – 5631	Beta – 427866	LC	
2013/12 3.82-3.83	Shell fragments	42150 ± 570	44666 – 42555	Beta – 427864	BC	Shell fragments presumably reworked based on date on bulk organics above them
2013/12 3.865-3.88	Bulk organics	25220 ± 100	27617 – 27011	Beta – 427863	BC	
2013/14 2.98-3.00	Bulk organics	10390 ± 30	10456 – 10142	Beta – 427861	LC	
2013/15 3.29-3.31	Bulk organics	11060 ± 50	11113 – 10841	Beta – 427862	LC	
2013/18 1.78-1.79	Bulk organics	10720 ± 40	10781 – 10644	Beta – 427859	LC	This sample and Beta – 427860 are from the same unit but sampled in different core segments
2013/18 2.15-2.165	Bulk organics	10490 ± 30	10611 – 10300	Beta – 427860	LC	
2013/19 1.65-1.66	Bulk organics	9760 ± 30	9289 – 9218	Beta – 436099	LC	This sample and Beta – 427865 are from the same unit but sampled in different core segments
2013/19 2.05-2.06	Bulk organics	8880 ± 30	8223 – 7948	Beta – 427865	LC	

*BC = Basal complex; LC = Lower complex. As noted in the text, it was not possible to obtain datable material from the Upper Complex

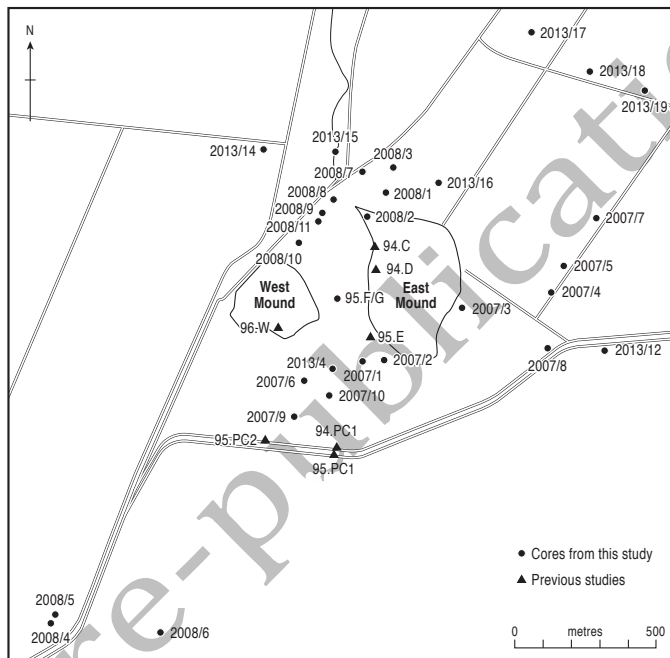
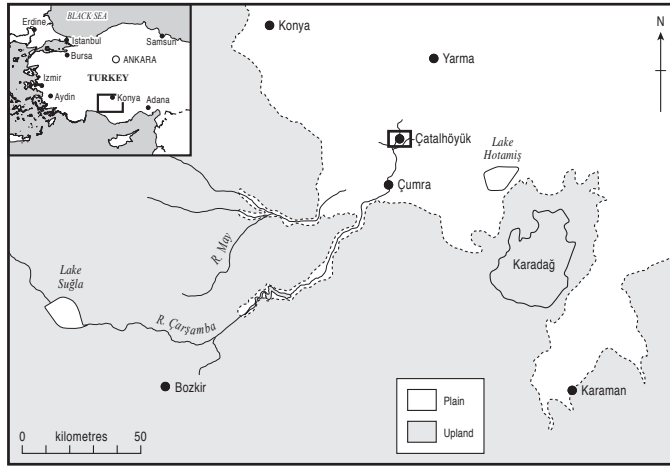


Figure 1.

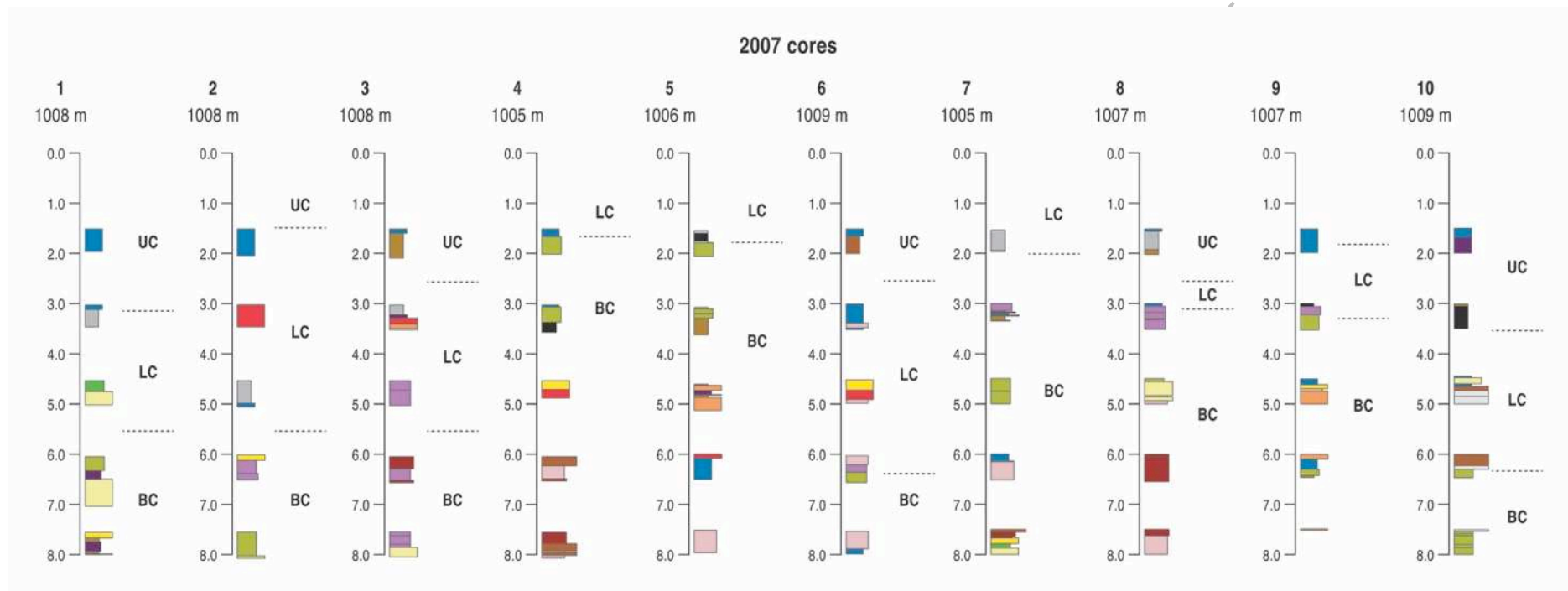


Figure 2a

Pre-public

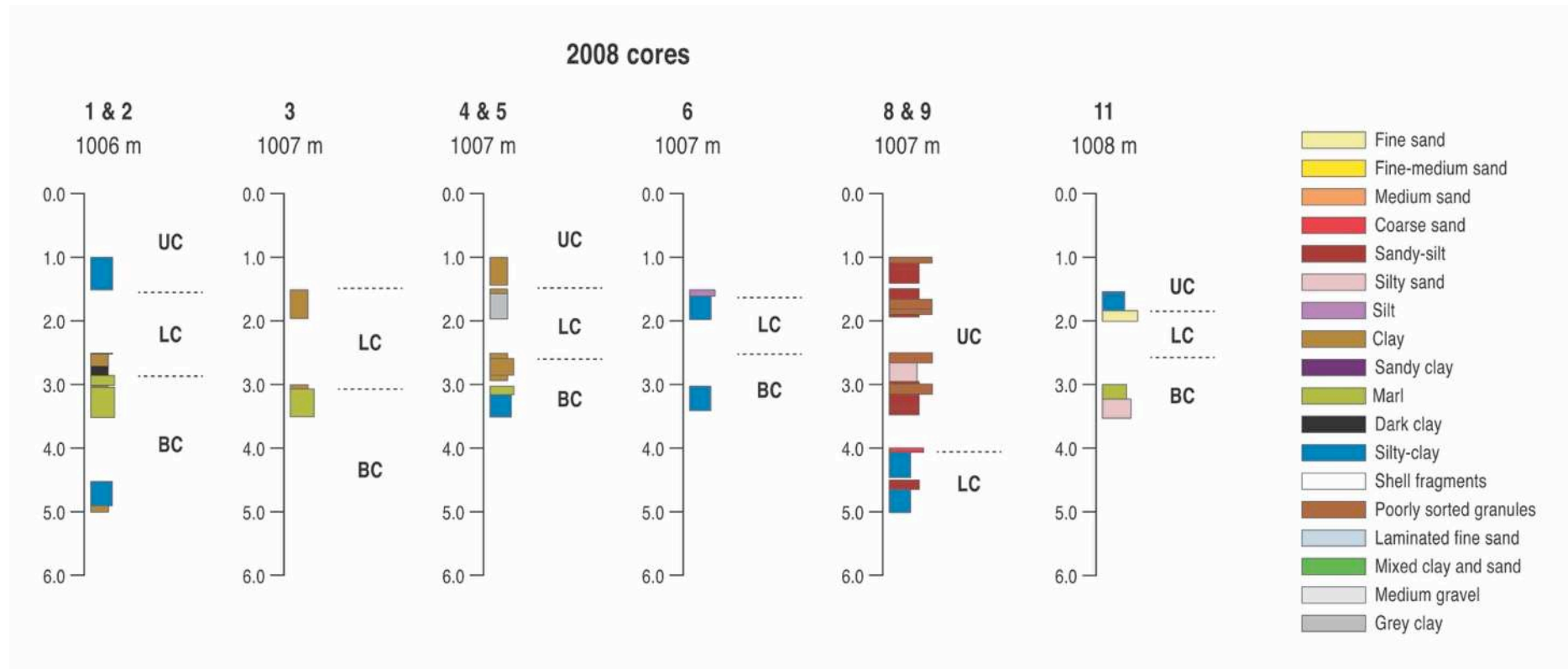


Figure 2b

Pre-pub

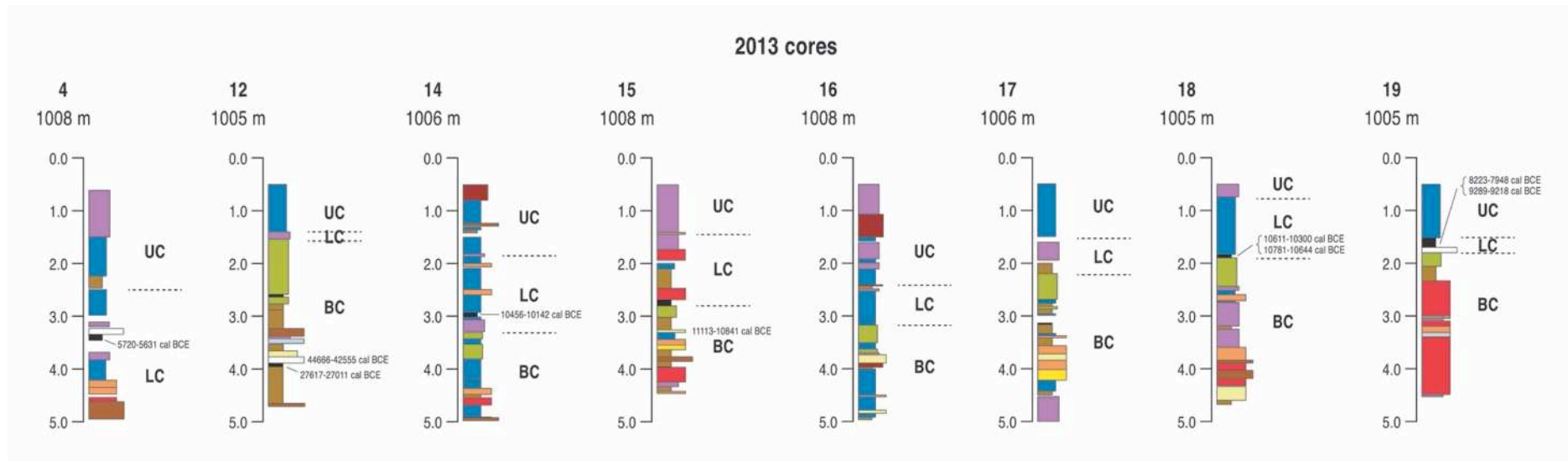


Figure 2c

Pre-publication

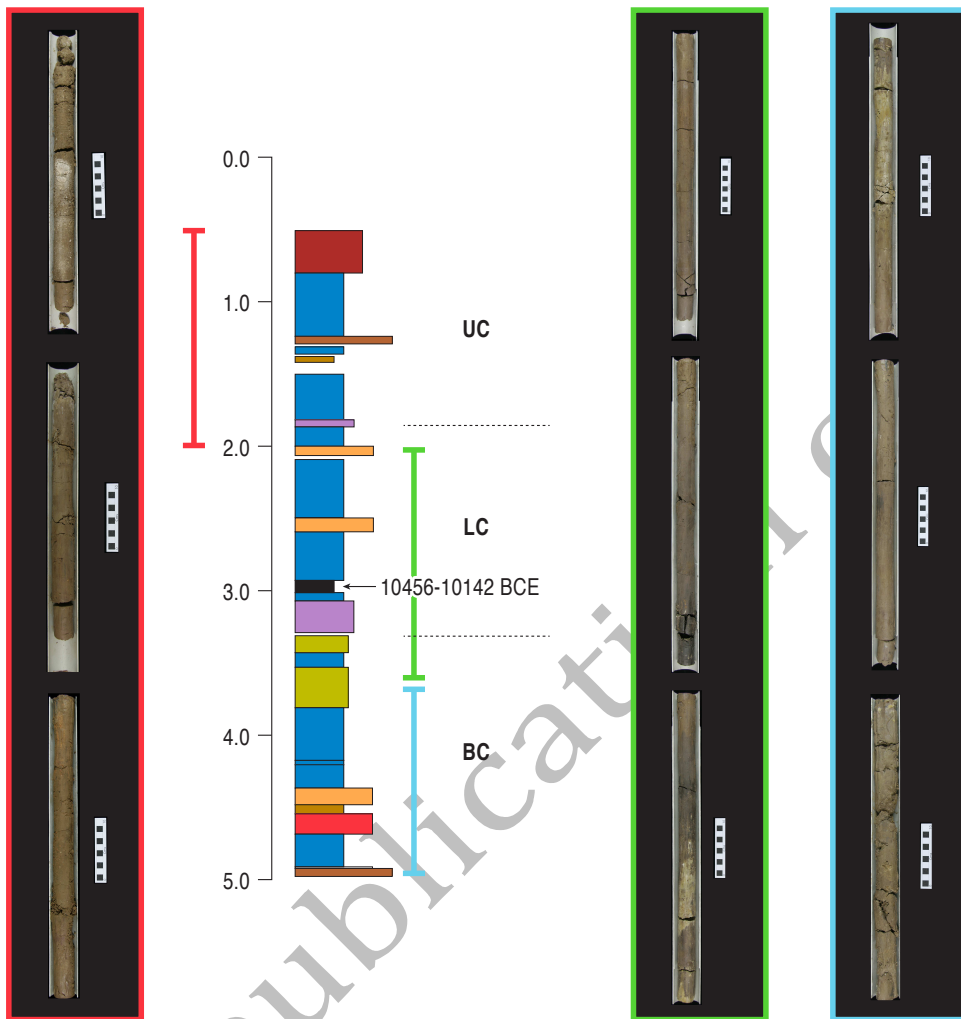


Figure 3

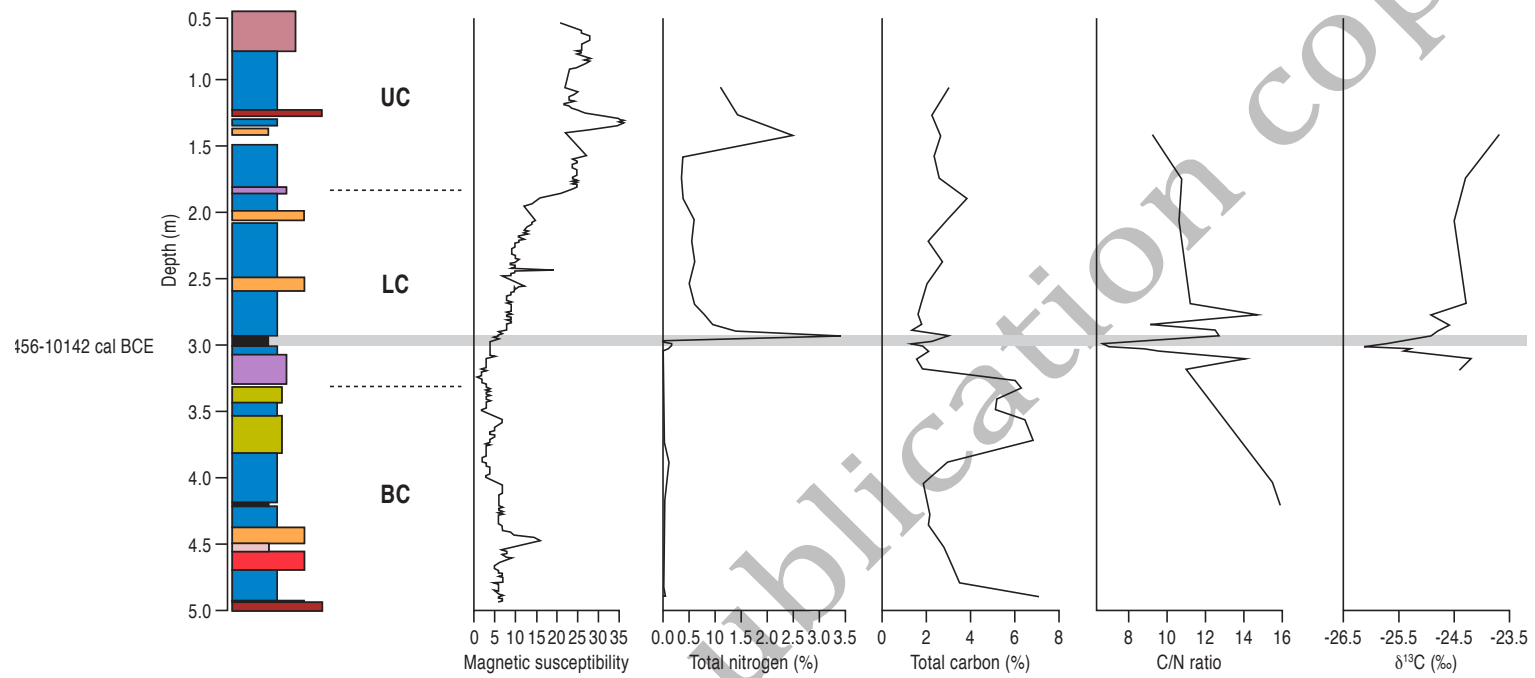


Figure 4

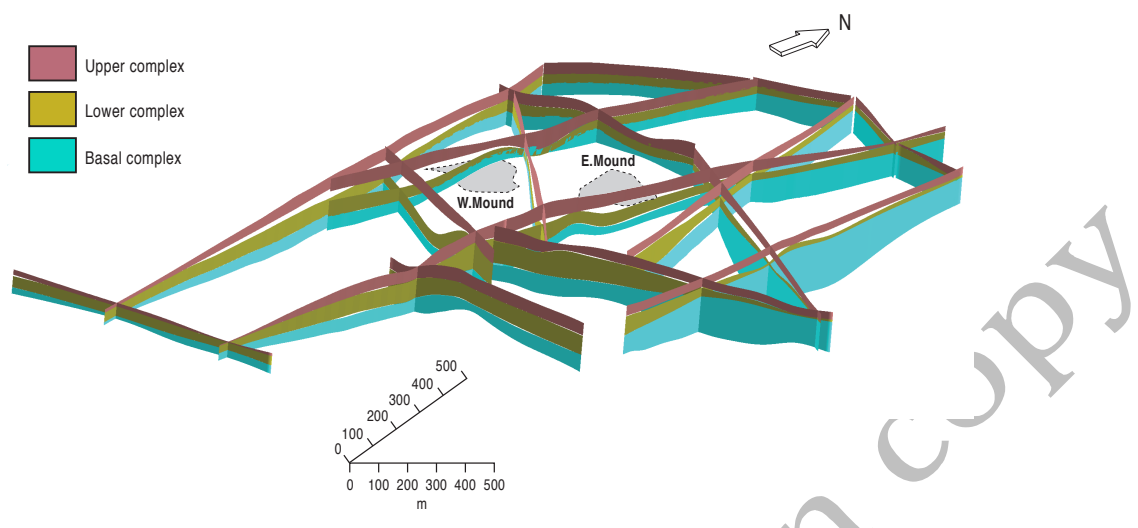


Figure 5

Pre-publication copy

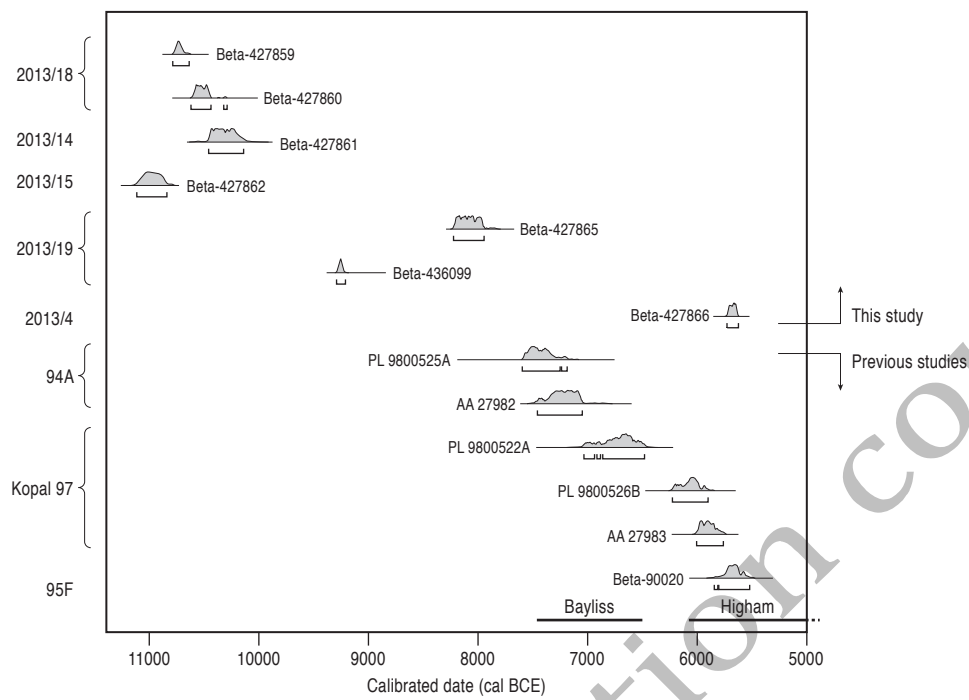


Figure 6

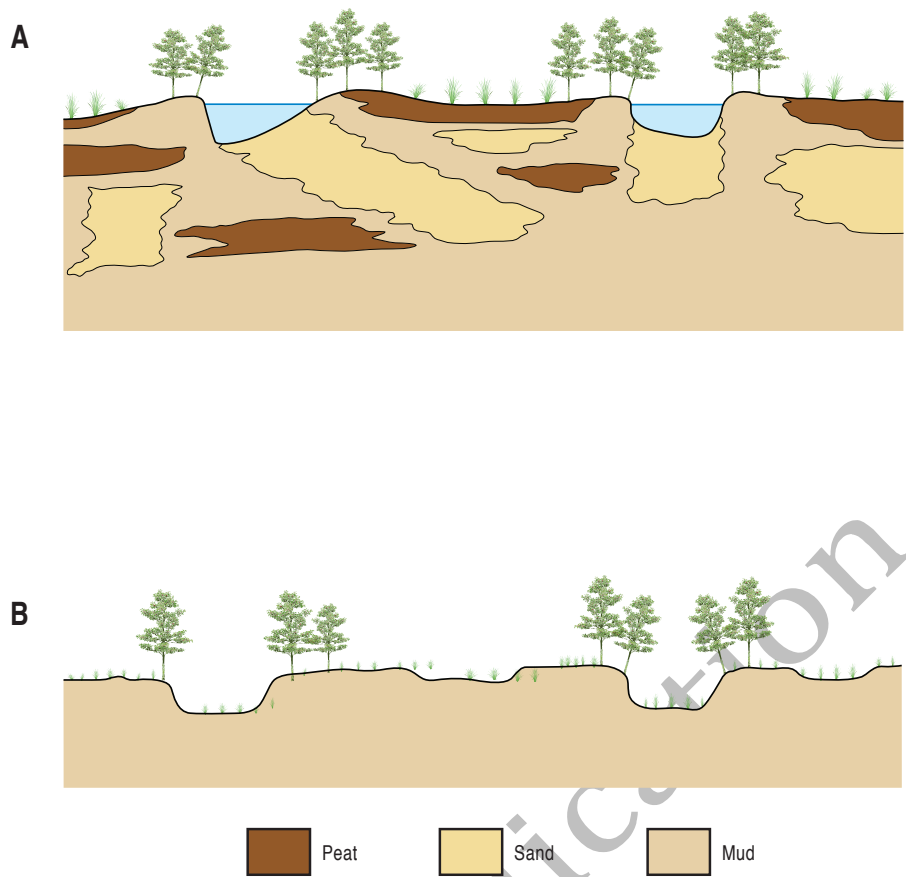


Figure 7

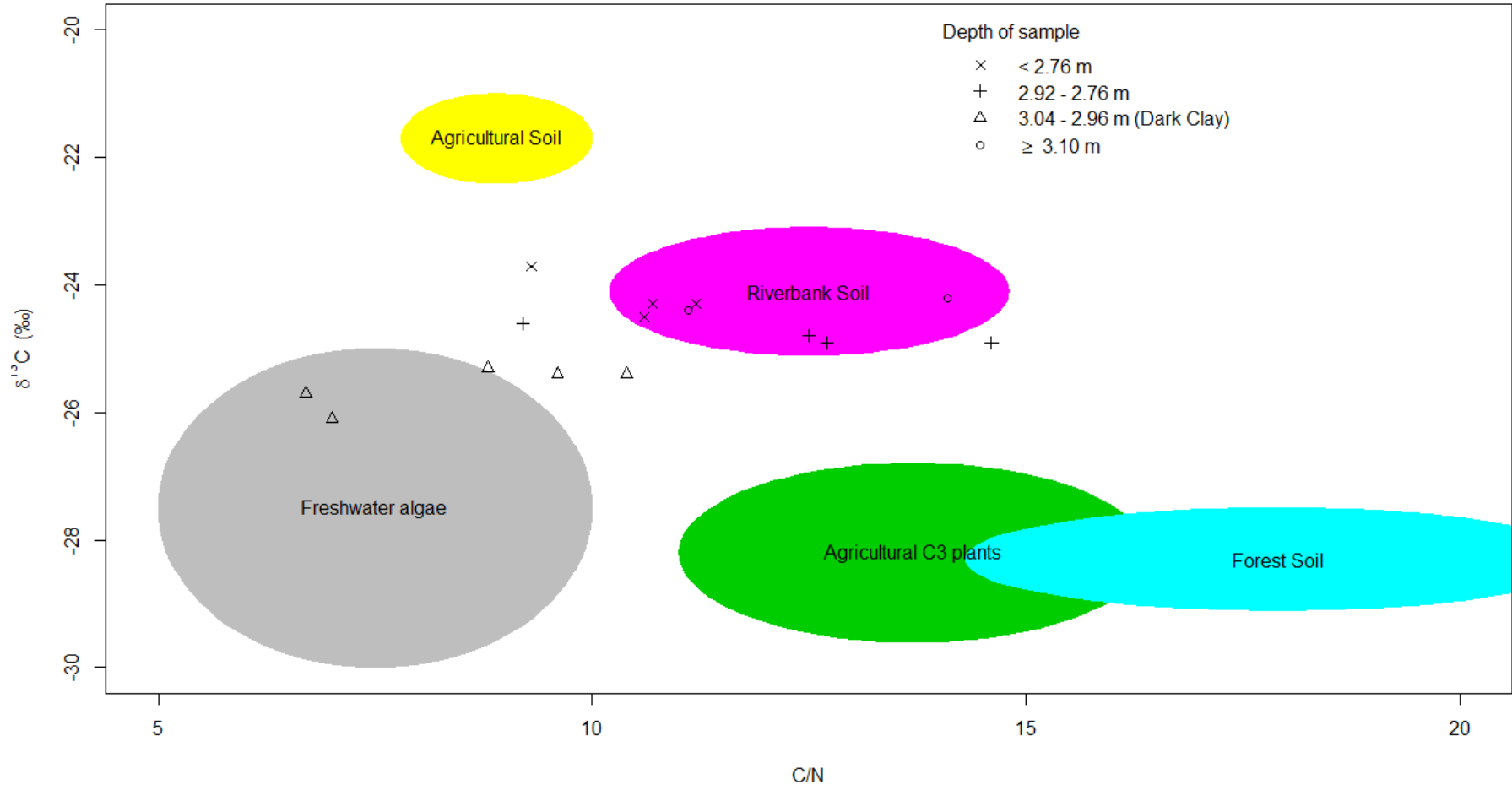


Figure 8

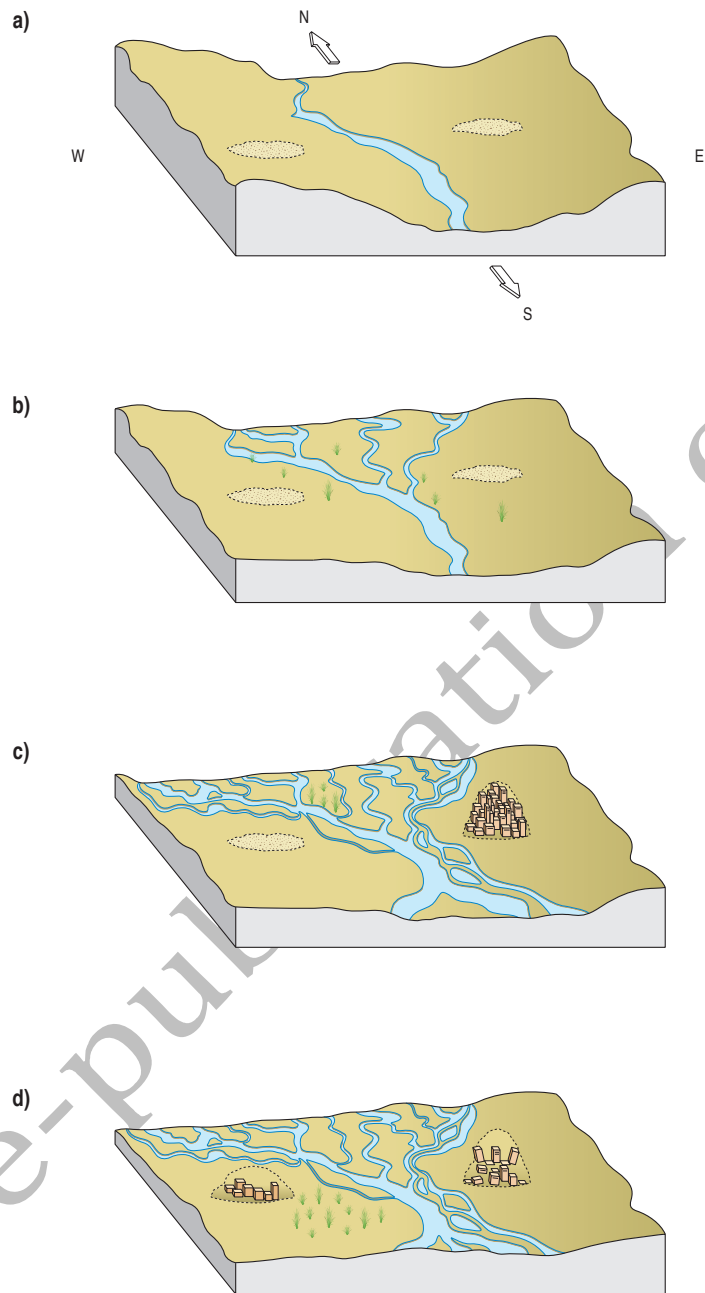


Figure 9